

Ab Initio SCF Calculations on the Photochemical Behavior of the Three-Membered Rings. 4. Oxirane: Fragmentation¹

B. Bigot, A. Sevin, and A. Devaquet*

Contribution from the Laboratoire de Chimie Organique Théorique,² Université Pierre et Marie Curie, 4 Place Jussieu, 75230 Paris Cedex 05, France. Received May 30, 1978

Abstract: The complete evolution of ethylene oxide by monomolecular processes is theoretically simulated according to the reactive scheme designed in the preceding paper. Various pathways are examined describing the most usual fragmentations: formation of ethylene and atomic oxygen in one- and two-step processes; formation of carbene and formaldehyde by direct two-bond scission or from evolution of intermediates I and II by CC and CO bond ruptures, respectively; acetaldehyde formation by hydrogen migration from intermediate I. A semiquantitative rationale is proposed for the overall thermal reactivity and the photochemical behavior in the first accessible singlet and triplet valence excited states.

In the preceding paper,¹ we have first outlined the main experimental results concerning the photochemical behavior of oxirane derivatives. Then the primary processes of oxirane ring opening by CO or CC bond rupture have been theoretically studied by an ab initio SCF-CI method.³ These ruptures lead to the formation of two open intermediates, I and II, respectively (Figure 1), which can either be trapped by 1,3-dipolar cycloadditions on unsaturated system⁴ or evolve by further fragmentations or rearrangements to yield various species such as ethylene, atomic oxygen, carbenic entities, acetaldehyde, carbon monoxide, methyl radical, etc.⁵

Since our general purpose is to provide a basis for a rationalization of oxirane monomolecular reactivity, we must now examine the complete evolution of the system from its initial structure to the most commonly formed fragments.

In order to get some new theoretical information on these transformations, we have simulated the following reaction paths: (1) direct extrusion of oxygen from oxirane by a simultaneous two-bond scission process (path 3); (2) fragmentation of the intermediate I into atomic oxygen and ethylene by a CO bond rupture (path 8); (3) direct extrusion of carbene from oxirane by a simultaneous two-bond scission (path 4); (4) fragmentation of the intermediate I into a carbenic entity (CH₂) and a formaldehyde molecule by CC bond rupture (path 6); (5) fragmentation of intermediate II into the same two products by CC bond rupture (path 5); (6) formation of acetaldehyde from intermediate I by migration of a hydrogen atom from one carbon to the other (path 7).

In our semiquantitative perspective, we have used the already well documented method which consists in minimal basis STO-3G⁶ calculations and CI treatment.⁷ To link the initial and final structures, we have assumed linear variations of the different geometrical parameters. All these points were developed in the preceding paper.¹

This procedure, associated with the minimal basis and the limited CI calculations, provides semiquantitative results which allow us to carry out qualitative conclusions of chemical significance, as already shown.^{1,3a,8}

We will now examine the various paths in detail.

Fragmentation into Ethylene Plus Atomic Oxygen

(1) Simultaneous Two-Bond Scission: Path 3. The simulated process was achieved assuming that a C_{2v} symmetry is preserved all through the reaction path. The final distance between the oxygen atom and the ethylene molecule was taken equal to 2.5 Å.

Let us first consider the behavior of the MOs (Figure 2). The three MOs n_z, n_x, and W_A, mainly concentrated on oxygen, tend to correlate respectively with the p_z, p_x, and p_y oxygen atomic orbitals. W_A* naturally correlates with π_{CC}* and W_S* with π_{CC}; a HOMO-LUMO crossing results, which is avoided

for symmetry reasons (dotted lines). Before drawing the subsequent correlation state diagram, it is necessary to define the electronic states of the final system: C₂H₄ + O.

The first ones correspond to ethylene in its ground state and to atomic oxygen in its 15 different configurations ³P, ¹D, ¹S. The following states are the familiar^{1,3} ππ* excited states of ethylene associated with atomic oxygen in various electronic states (Figure 3).

According to the MO scheme, oxirane ground state (GS) correlates directly to C₂H₄ (GS) + O (¹D) while the ^{1,3}n_z W_A* states tend to correlate with high-lying charge transfer states: C₂H₄⁻ + O⁺, the ^{1,3}n_z W_S* states with C₂H₄ (GS) + O (³P), and the ^{1,3}n_x W_A* states with C₂H₄ (^{1,3}ππ*) + O (¹D).

At the end of the path, the degenerate oxygen states—which are only slightly splitted by residual interaction with the ethylenic system—correspond, at the CI level, to complex wave functions whose natural counterparts in the initial oxirane are nonrealistic high-lying polyexcitations. Consequently, several crossings occur, such as along the ^{1,3}n_z W_A* or ^{1,3}n_x W_A* correlations, but they are masked by the fast descent of the potential energy curves (PECs) and do not appear to be of chemical importance.

The calculated PECs confirm this analysis (Figure 4). There is no maximum on the GS PEC, but its convex shape is due to the avoided crossing solved at the MO level.⁸ The energy difference between initial and final systems (ΔE ≈ 106 kcal/mol) prevents this thermal fragmentation from occurring under usual reactive conditions.

On the other hand, the reverse reaction (formation of oxirane from atomic oxygen in its ¹D state and ethylene (GS)) seems very easy, in agreement with the experimental works dealing with this oxygen singlet state.⁹

All the excited states PECs are sharply descending, and thus, whatever the populated excited state, the fragmentation is very easy, yielding the stable O (³P) + C₂H₄ (GS) system. The crossing of the triplet and GS PECs (points B, C, and D) can reduce the efficiency of the process since intersystem crossing allows the reclosure to oxirane.

Conversely, atomic oxygen in its triplet ³P state can add to C₂H₄ (GS), after overcoming an energy barrier (≈ 23 kcal/mol) and an intersystem crossing (point B or C). The oxirane formation in this process is thus more difficult in the triplet than in the singlet state.

(2) Two-Step Oxygen Extrusion: Path 1 + Path 8. To simulate this process, we have assumed that the ring opening by CO cleavage leading to intermediate I (path 1) is followed by elongation of the remaining CO bond, up to a final CO distance of 3.2 Å (path 8) along its valence axis.

The part corresponding to path 1 has already been studied in the preceding paper.¹ Let us first consider the behavior of the molecular orbitals during path 8: p₊ tends to correlate

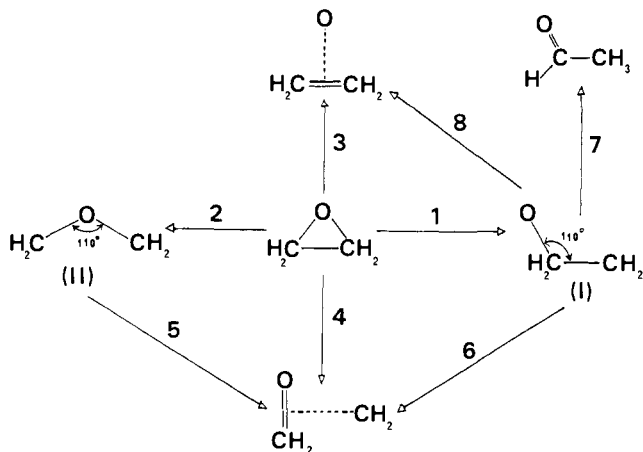


Figure 1. Scheme presenting the different reaction paths of the oxirane and related systems presently studied.

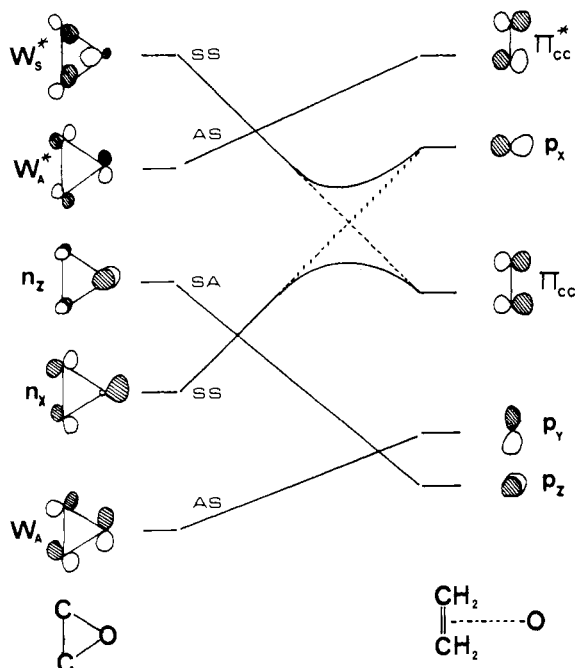


Figure 2. MO correlation diagram in the simultaneous two-bond scission of oxirane to ethylene plus atomic oxygen (path 3). The symmetry symbols S or A refer to the two symmetry planes conserved in the process.

naturally with p_x , p_y with π^*_{CC} , $\sigma^*_{CH_2}$ with π_{CC} . All these orbitals have the same symmetry characteristics and all the crossings are avoided, as shown in Figure 5. The state correlations which then follow are complex. Indeed, the four low-lying $1,3D_{\sigma\sigma}$ and $1,3D_{\sigma\pi}$ states mix various configurations, the ones intending to correlate with high-lying charge transfer states, the others to C_2H_4 (GS) + O ($1D$ or $3P$). Then, at state level, the same reasons as in the preceding case (see Figure 3) add to the consequences of the avoided crossing of the MO pattern. As a result, the calculated PECs shapes (Figure 6) reflect these different kinds of avoided crossings. Various conclusions can, however, be carried out.

Thermally, this fragmentation appears very unlikely. The overall process—which in fact does not involve the formation of an intermediate—would need the overcoming of an important activation barrier (105 kcal/mol), very similar to that of the one-step process.

The reverse reaction, addition of oxygen O ($1D$) to ethylene (GS), is easier in the one-step process ($\Delta E \approx 0$ kcal/mol) than in the present two-step reaction ($\Delta E \approx 8$ kcal/mol). However, the calculations allow us to predict that, at any rate, no dis-

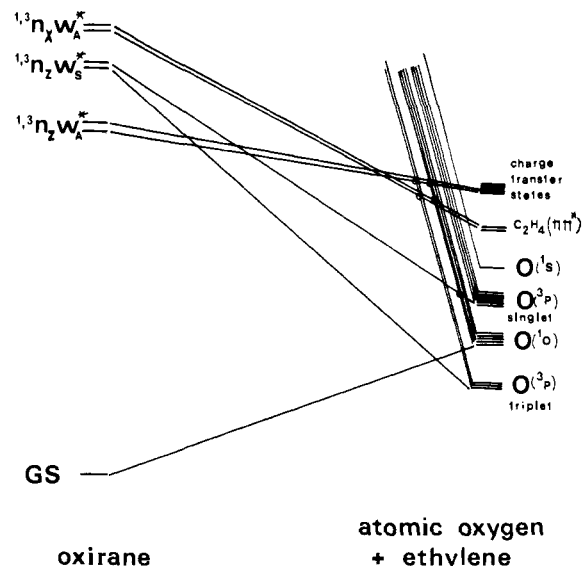


Figure 3. State correlation diagram in the simultaneous two-bond scission of oxirane to ethylene plus atomic oxygen (path 3). The circles on the correlation lines mean an avoided crossing for symmetry reasons.

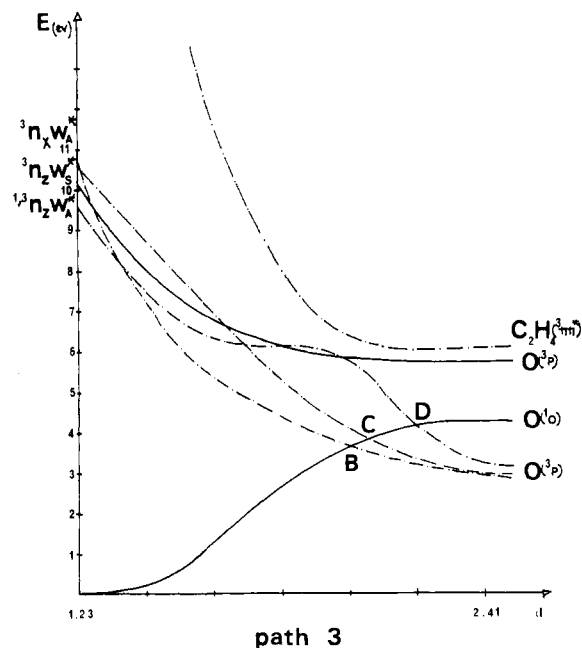


Figure 4. Calculated potential energy curves in the simultaneous two-bond scission of oxirane to ethylene plus atomic oxygen (path 3). The dotted lines are relative to the triplets and the full lines to the singlets. d represents the distance between oxygen atom and the CC bond middle.

tingtion can be experimentally made between these two possibilities, since no stable intermediate is formed during the singlet addition.

Photochemically, we have already seen that path 1 is spontaneous either in the triplet or singlet states. It leads to the $1,3D_{\sigma\pi}$ or $1,3D_{\sigma\sigma}$ states of I, which appears to be a quite stable intermediate. The sharp decrease of their corresponding PECs ($\Delta E \approx 160$ kcal/mol) allows the system to accumulate sufficient internal energy for overcoming the energy barrier of the second step ($\Delta E \approx$ kcal/mol for $3D_{\sigma\sigma}$ or $3D_{\sigma\pi}$, $\Delta E \approx 80$ kcal/mol for $1D_{\sigma\pi}$).

Let us note that, since intermediate I can have a nonnegligible lifetime in its $1,3D_{\sigma\pi}$ or $3D_{\sigma\sigma}$ states, another channel must be considered. This is decay, by internal conversion to $1D_{\sigma\sigma}$ state and spontaneous reclosure to oxirane (GS).

The reverse addition of triplet atomic oxygen to C_2H_4 in-

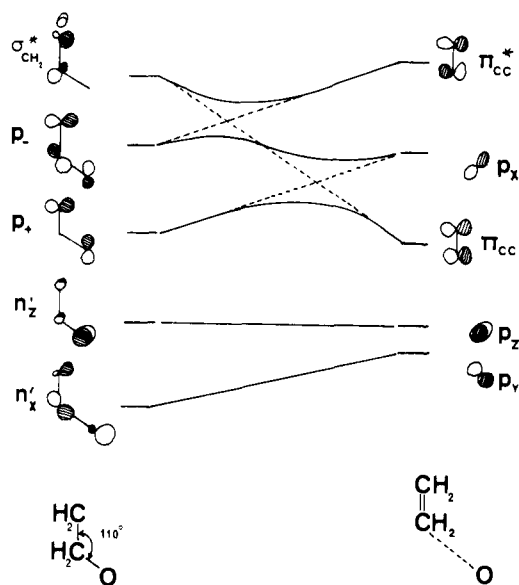


Figure 5. MO correlation diagram in formation of atomic oxygen plus ethylene from intermediate 1 (path 8).

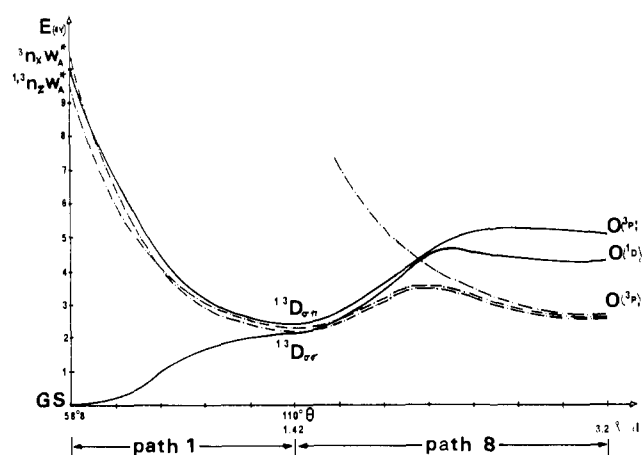


Figure 6. Calculated potential energy curves in the two-step rupture of oxirane to ethylene plus atomic oxygen (path 1 + path 8). The left part of the figure is relative to path 1 and the right one to path 8. θ represents the OCC angle and d the CO distance. The dotted lines are relative to the triplets and the full lines to the singlets.

volves the overcoming of a barrier (18 kcal/mol) comparable to the one found in the one-step approach. However, in the two-step process, there is no need of intersystem crossing to reach the stable intermediate which can easily decay to oxirane GS. This situation appears more favorable, in good agreement with experimental evidence since the intermediate I has already been detected in the addition reaction of oxygen to ethylene^{9,10} Moreover, a sufficient stability of the triplet intermediate allows us to predict a stereochemical randomization during this addition process.

Carbene Formation

Following Figure 1, three different reactive paths can be considered. The first one is a synchronous two-bond rupture (path 4). The second and third ones are two-step processes involving first ring opening (path 1 or path 2) followed by fragmentation of the resulting intermediates (paths 6 and 5, respectively).

(1) **Simultaneous Two-Bond Scission: Path 4.** To simulate this reaction, we have assumed that the CH_2 group moves along a direction perpendicular to the CO bond. The final distance between the CH_2 entity and the middle of the CO

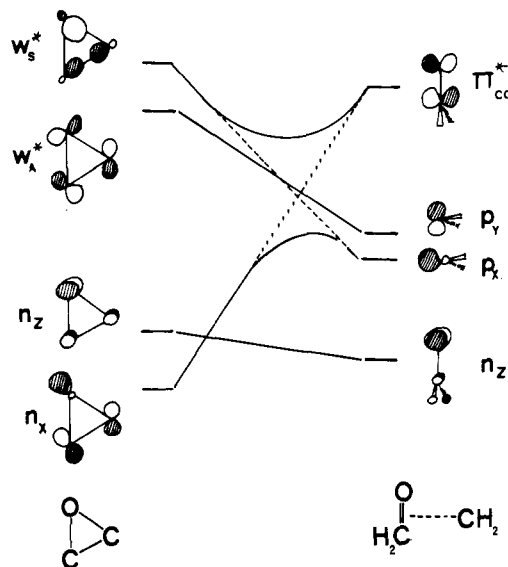


Figure 7. MO correlation diagram in the simultaneous two-bond scission of oxirane to formaldehyde plus methylene (path 4).

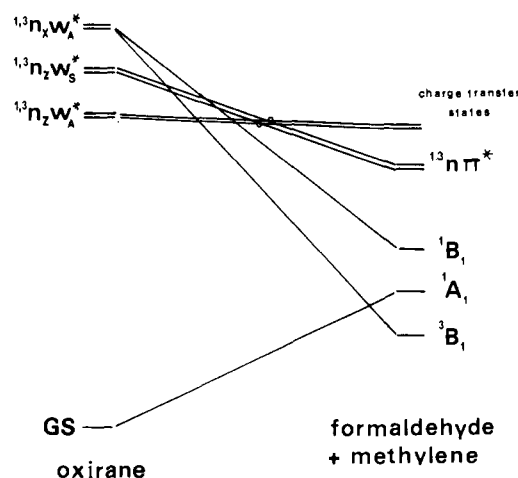


Figure 8. State correlation diagram in the simultaneous two-bond scission of oxirane to formaldehyde plus methylene (path 4). The circles on the correlation lines mean an avoided crossing.

bond is 3.0 Å. The HCH angle of the methylene group was kept constant at its initial value: 115.5°. It is an intermediate value between the optimal values of 102.4° for the 1A_1 state and 134.0° for the 3B_1 state of methylene.¹¹

The MO correlation diagram (Figure 7) exhibits various avoided crossings. They come from the fact that all considered MOs, except n_z , have the same symmetry characteristics. Naturally, n_x would tend to correlate with π^*_{CO} , W_A^* with p_y , and W_S^* with p_x (dotted lines). Once solved in the SCF step of the calculations, the full line correlations are observed.

As in the case of oxygen extrusion, the state correlation diagram (Figure 8) is rather complex. In agreement with the MO pattern, the oxirane GS correlates with H_2CO (GS) + CH_2 (1A_1), the $1,3n_z W_A^*$ states with high-lying charge transfer states ($\text{H}_2\text{CO}^+ + \text{CH}_2^-$), the $1,3n_z W_S^*$ states with H_2CO ($1,3n\pi^*$) + CH_2 (1A_1), and the $1,3n_x W_A^*$ states with H_2CO (GS) + CH_2 ($1,3B_1$). Two avoided crossings result, concerning the $1,3n_z W_A^*$ and $1,3n_z W_S^*$ states.

The calculated PECs, although qualitatively in fair agreement with the preceding analysis, exhibit typical features which deserve some more comments (see Figure 9). First, on the GS PEC, a neat maximum appears in relation with a deep minimum on the $1n_x W_A^* \leftrightarrow ^1B_1$ curve. It is a remnant of the strong

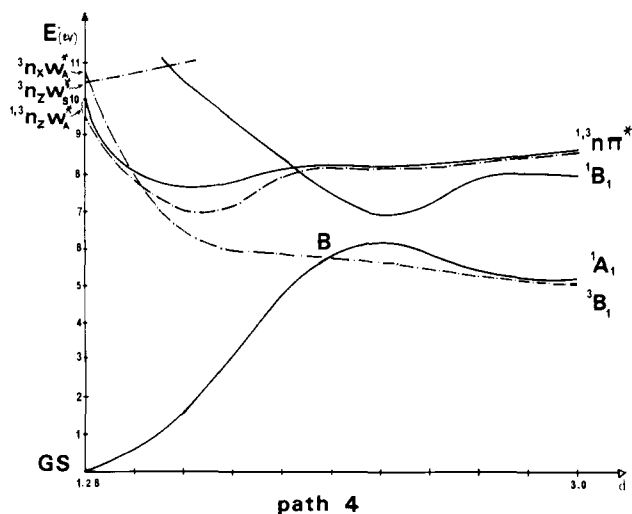


Figure 9. Calculated potential energy curves in the simultaneous two-bond scission of oxirane to formaldehyde plus methylene (path 4). The dotted lines are relative to the triplets and the full lines to the singlets. d represents the distance between the methylene carbon atom and the CO bond.

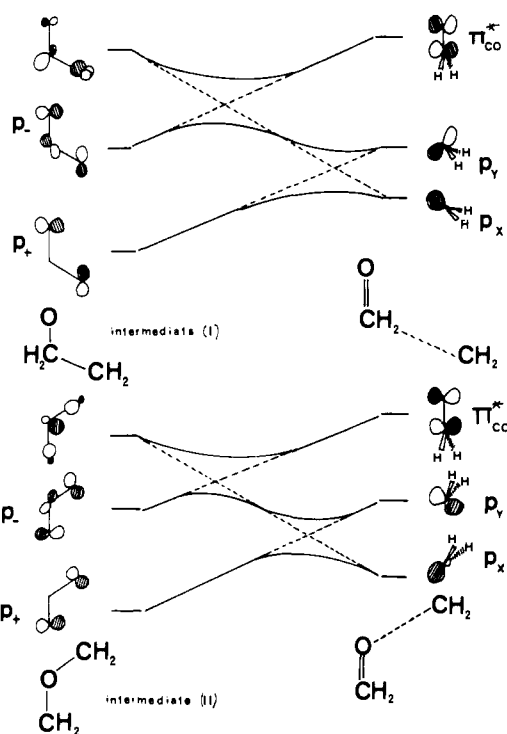


Figure 10. (Above) MO correlation diagram in the formation of methylene plus formaldehyde from intermediate I (path 6). (Below) MO correlation diagram in the formation of methylene plus formaldehyde from intermediate II (path 5). The dashed lines are relative to the natural correlations and the full lines to the SCF correlation.

avoided crossing found at the MO level.⁸ On the other hand, the minima on the $^{1,3}n_z W_A^*$ PEC are unexpected since no potentially repelling states are found at lower energy, and the state diagram rather allows us to foresee maxima. The reason is again found at the MO natural correlation level; at the beginning of the motion, W_A^* is strongly stabilized and the $^{1,3}n_z W_A^*$ states go down; but soon, the fragmentation into two distinct groups induces a charge transfer situation and the corresponding PECs go up.

The following conclusions derive from Figure 9.

(1) Thermally the fragmentation reaction into H_2CO (GS) and CH_2 (1A_1) is impossible, the corresponding activation energy being 140 kcal/mol. The reciprocal addition of meth-

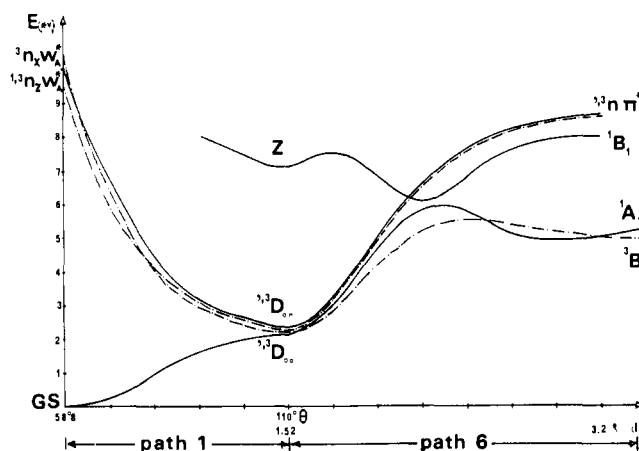


Figure 11. Calculated potential energy curves in the two-step rupture of oxirane to formaldehyde plus methylene (path 1 + path 6). The left part of the figure is relative to path 1 and the right one to path 6. θ represents the OCC angle and d the CC distance. The dotted lines are relative to the triplets and the full lines to the singlets.

ylene (1A_1) to formaldehyde involves the overcoming of a 22 kcal/mol energy barrier. We will later compare this value to the ones encountered in the two-step processes.

(2) Photochemically, different reactive channels must be examined. The easiest would consist in populating, if possible, the $^3n_x W_A^*$ state leading directly to CH_2 (3B_1) + H_2CO (GS). An intersystem crossing (point B, Figure 9) can reduce the efficiency of the process by providing a leak to reclosure into oxirane.

The population of the $^{1,3}n_z W_A^*$ states either leads directly to CH_2 (1A_1) + H_2CO ($^{1,3}n\pi^*$) or induces the formation of an exciplex-like species in the vicinity of their PEC minimum. The first occurrence is more likely in the singlet, and the second in the triplet. The "exciplex" can decay either to oxirane GS or to the reactive, near-touching, PEC $^3n_x W_A^*$ which leads to CH_2 (3B_1).

Addition of CH_2 (3B_1) to formaldehyde requires an activation barrier (12 kcal/mol) to reach point B, where an effective intersystem crossing can occur.¹²

Let us examine now the two-step procedures.

(2) **Two-Step Procedures.** Two reaction paths can be considered. The first one is the ring opening by CO rupture (path 1) and subsequent CC rupture (path 6). In the second one, the chronological bond rupture order is inverted (path 2 + path 5).

The MO correlation diagrams have the same features in the two cases and are very similar to that of path 8 already studied (Figure 5). They are represented in Figure 10. These two reaction paths (6 and 5) lead to the same type of complex state correlation diagrams as in path 8.

The corresponding calculated PECs are drawn in Figures 11 and 12. Let us first examine Figure 11.

Thermally the fragmentation reaction appears quite unlikely, the necessary activation energy being 136 kcal/mol. Photochemically, two reaction paths seems to be possible. The first one is to populate the $^3n_x W_A^*$ state. Spontaneously, the CO rupture occurs and leads to the formation of intermediate I in the stable $^3D_{\sigma\sigma}$ state. During this process, the system stores sufficient internal energy ($\Delta E \approx 160$ kcal/mol) for overcoming the energy barrier of the second step (78 kcal/mol) leading to CH_2 (3B_1) + H_2CO (GS). The second one is to populate the $^{1,3}n_z W_A^*$ states which here again lead spontaneously to the formation of intermediate I. The resulting electronic states $^{1,3}D_{\sigma\sigma}$ are not directly reactive, but, by internal conversion, the system can reach the $^3D_{\sigma\sigma}$ state and fragment into CH_2 (3B_1) + H_2CO (GS). An ultimate way consists in the

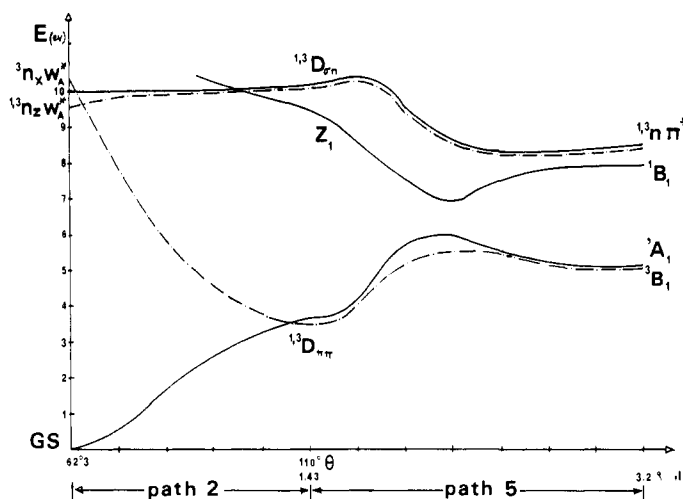


Figure 12. Calculated potential energy curves in the two-step rupture of oxirane to formaldehyde plus methylene (path 2 + path 5). The left part of the figure is relative to path 2 and the right one to path 5. θ represents the COC angle and d the CO distance. The dotted lines are relative to the triplets and the full lines to the singlets.

conversion into the $^1D_{\sigma\sigma}$ and the reclosure into oxirane, which lowers the efficiency of the process.

Let us examine now Figure 12.

Thermal fragmentation appears here again quite unlikely. The necessary activation energy is 142 kcal/mol, 6 kcal/mol more than in the preceding case. Photochemically, the $^3D_{\sigma\sigma}$ diradical intermediate II can be easily reached as already seen in the study of the CC rupture ring opening.¹ It will normally possess sufficient internal energy to overcome the 41 kcal/mol energy barrier which leads to CH_2 (3B_1) + H_2CO (GS).

To conclude this part, we will now examine the addition of CH_2 to formaldehyde. Let us consider first the singlet addition. Energetically, it is not possible to distinguish between the three procedures, since the energy barriers are in each case in the 20 kcal/mol range.

In the triplet addition, the one-step process implies an activation energy of 12 kcal/mol and an unfavorable intersystem crossing (point B, Figure 10). The two-step processes are easier; in both cases, an activation energy of 10 kcal/mol must be overcome. The intermediates I and II are then directly formed. After intersystem crossing to the $^1D_{\sigma\sigma}$ state, they reclose to oxirane. The intermediates I and II have certainly sufficient lifetime for allowing stereochemical scrambling.

Acetaldehyde Formation: Path 1 + Path 7

To simulate this complex rearrangement, we had to choose between several possibilities. We then assumed a motion sequence which allows a close connection with preceding reactive channels.

The corresponding geometrical transformations can be decomposed into two steps. The first one is the CO rupture ring opening (path 1) and the second is the migration of one hydrogen from the central carbon to the extremal one. This step has been optimized since no clear geometrical constraints can a priori be proposed as a guide.

The resulting calculated PECs are drawn in Figure 13. The left part of the drawing corresponds to the now familiar ring opening and the right part to hydrogen migration.

The absence of any symmetry element implies that there are no crossings between PECs of the same spin multiplicity. Thus the $^1D_{\sigma\sigma}$ state of intermediate I correlates with the ground state of acetaldehyde, $^1,^3D_{\sigma\pi}$ with $^1,^3n\pi^*$, and $^3D_{\sigma\sigma}$ with $^3\pi\pi^*$.

Thermally, this intramolecular reaction is difficult since it requires the overcoming of a 92 kcal/mol energy barrier. Nevertheless, the activation energy necessary to cleave in a first

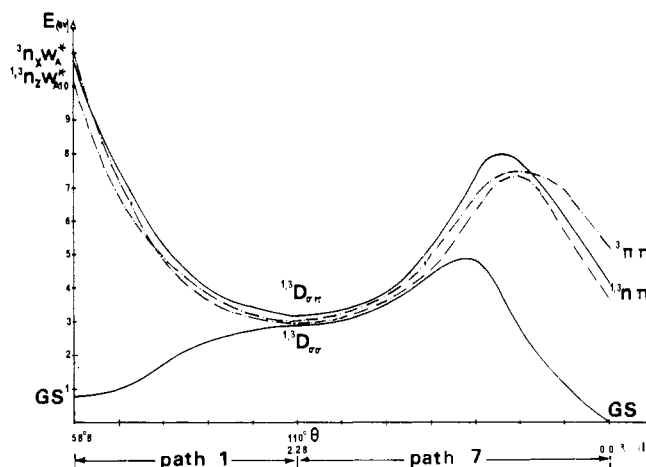


Figure 13. Calculated potential energy curves in the two-step process of formation of acetaldehyde from oxirane (path 1 + path 7). The left part of the figure is relative to path 1 and the right part to the hydrogen migration (path 7). The abscissa of the second step is relative to the migrating hydrogen normal projection on the CC bond. The dotted lines are relative to the triplets and the full lines to the singlets.

step the CO linkage (45 kcal/mol) lies satisfactorily within the range of experimental findings. The overall process (experimental activation energy 57 kcal/mol)^{5d,g} is not properly described by our simulation, thus comforting the assumption that an intermolecular radical chain process is likely to take place once the CO bond is broken.

The related photochemical process is easier. The population of $^1,^3n_z W_A^*$ or $^3n_x W_A^*$ leads to the formation of intermediate I ($^1,^3D_{\sigma\pi}$, $^3D_{\sigma\sigma}$). The migration in the $^1,^3D_{\sigma\pi}$ or $^3D_{\sigma\sigma}$ states involves energy barriers in the 110 kcal/mol range, and appears nonrealistic, even if the system has conserved, as internal energy, a large part of the 160 kcal/mol corresponding to the potential energy variation during the first process. However, owing to the energetic degeneracy of the different states of intermediate I, the system can reach the $^1D_{\sigma\sigma}$ state and either reclose to oxirane or evolve to acetaldehyde. In this case, the 40 kcal/mol barrier involved in the migration can easily be overcome, considering the internal energy accumulated during the ring opening.

The resulting acetaldehyde molecule is in its ground state, but certainly possesses an important amount of internal energy. This is a "hot species" which can undergo further evolution such as CC breaking to yield the fragments $\text{HCO} \cdot + \text{CH}_3 \cdot$, which are indeed experimentally detected.⁵

Conclusion

Various competing processes are involved in oxirane reactivity. Starting from the initial molecule, formaldehyde formation is exothermic (-19 kcal/mol, calculated¹⁴ -27 kcal/mol), while the other processes are endothermic: formation of ethylene plus oxygen (75 kcal/mol, calculated 84 kcal/mol), formation of formaldehyde plus carbene (88 kcal/mol, calculated 70-80 kcal/mol).¹⁴ These results illustrate the accuracy of minimal basis set calculations which are known to slightly favor too much compact structures over separated fragments.

Thermally, all reactive paths seem hard to reach. Either the activation energy is too high (96 kcal/mol for disrotatory CC opening, 90 kcal/mol for the conrotatory mode, 92 kcal/mol for the formation of acetaldehyde, 106 kcal/mol for oxygen extrusion in a two-step process, 140 kcal/mol for expulsion of carbene whatever the considered path), or no minimum is found along the corresponding PECs (face to face CC ring opening, CO opening, one-step oxygen extrusion).

All these results clearly reflect the exceptional thermal

stability of the oxirane ring. Keeping in mind that our results are only semiquantitative, it is difficult to compare the calculated values to the available experimental ones^{5g} which refer to the GS thermal reactivity. Moreover, most of the experimental activation energies are given for overall processes and do not allow us to depict each step of a given reaction path (see the preceding remark relative to acetaldehyde formation). For these reasons, a comparison of the relative reaction facilities from our calculations may only afford a scale which is thus an upper limit to the real behavior of the system.

Photochemically, the analysis is much more complex. Let us first sum up the possibilities in the case of the population of $^1n_z W_A^*$.

The easiest primary reaction is the ring opening by CO rupture. Two other possible, but less probable, primary reactions are the expulsion in one step of carbene or of atomic oxygen. In these two cases, the final system is not in its more stable state ($CH_2(^1A_1) + CH_2O(^1\pi\pi^*)$ and $O(^3P) + C_2H_4$ (GS), respectively). Thus it can undergo various evolutions which can reduce the efficiency of such processes.

At last, we find the various modes of CC opening. They involve an effective intersystem crossing with the reactive $^3n_z W_A^*$ PEC (face to face or conrotatory mode) or lead directly to the high-lying zwitterionic Z_1 state (disrotatory mode).

From the CO rupture ring opening, already considered, various reactive channels appear, keeping in mind that the resulting intermediate (I) possesses a great amount of internal energy.

If the system remains in its $^1D_{\sigma\sigma}$ state, all evolutions are difficult: the oxygen departure in its 3P singlet state requires 70 kcal/mol, the hydrogen migration to form acetaldehyde ($^1n\pi^*$), 106 kcal/mol, and the carbene departure, 140 kcal/mol.

If, by internal conversion, the system converts to the degenerate $^1D_{\sigma\sigma}$ state, four channels must be considered. The reclosure to oxirane involves no energy barrier, the formation of acetaldehyde requires 42 kcal/mol, the oxygen departure ($O(^1D)$), 56 kcal/mol, and the carbene expulsion ($CH_2(^1A_1)$), 86 kcal/mol.

If, by intersystem crossing, the degenerate $^3D_{\sigma\sigma}$ state is populated, the oxygen departure ($O(^3P)$) involves only 33 kcal/mol.

Now let us consider the case of population of $^3n_z W_A^*$. Three primary processes will compete: the CO opening, the CC disrotatory mode opening, and the one-step oxygen expulsion. The first one can easily evolve toward oxygen expulsion (33 kcal/mol), less easily toward carbene formation (82 kcal/mol) or toward acetaldehyde formation (100 kcal/mol). The second can evolve toward carbene expulsion (46 kcal/mol). The one-step fragmentation into C_2H_4 (GS) + $O(^3P)$ involves no energy barrier.

The last possibility to be considered is the population of $^3n_x W_A^*$. The CO opening remains as easy as in the case of $^3n_z W_A^*$ population and leads to the same possible evolutions. The CC rupture ring opening, either face to face or in the disrotatory mode, are competitive as well as the direct expulsion of carbene ($CH_2(^3B_1)$) or atomic oxygen ($O(^3P)$). This is the least selective excited pathway.

In conclusion, these results clearly illustrate the following experimental facts. For oxirane derivatives bearing substituents which do not stabilize zwitterionic forms, CO bond rupture is the most effective primary process. The major secondary processes are either oxygen departure or acetaldehyde formation, which are in strong competition with the noneffective reclosure of the cycle.

For the other oxirane derivatives, CC bond rupture competes and leads to products less susceptible to reclose. They can either be trapped by 1,3-dipolar cycloaddition or fragment into a carbenic entity and carbonyl compounds.

References and Notes

- (1) B. Bigot, A. Sevin, and A. Devaquet, *J. Am. Chem. Soc.*, preceding paper in this issue.
- (2) This laboratory is associated with CNRS (ERA no. 549).
- (3) (a) For a detailed description of the method, see B. Bigot, A. Sevin, and A. Devaquet, *J. Am. Chem. Soc.*, **100**, 2639 (1978). (b) W. J. Hehre, W. A. Lathan, R. Ditchfield, M. D. Newton, and J. A. Pople, QCPE, No. 236, Indiana University, Bloomington, Ind.
- (4) R. Huisgen Symposium de Chime Heterocyclique, Universite de Mons, Sept 26-27, 1974; R. Huisgen, *Angew. Chem., Int. Ed. Engl.*, **2**, 565 (1963); **16**, 572 (1977).
- (5) (a) R. Gomer and W. A. Noyes, *J. Am. Chem. Soc.*, **72**, 101 (1950); (b) R. J. Cvetanovic, *Can. J. Chem.*, **33**, 1684 (1955); R. J. Cvetanovic and L. C. Doyle, *ibid.*, **35**, 605 (1957); (c) G. Flemming, M. M. Anderson, A. J. Harrison, and L. W. Pickett, *J. Chem. Phys.*, **30**, 351 (1959); (d) S. W. Benson, *ibid.*, **40**, 105 (1964); (e) M. Kawasaki, T. Ibuki, M. Iwasaki, and J. Takesaki, *ibid.*, **59**, 2076 (1973); (f) M. R. Bertonniere and G. W. Griffin, "Organic Photochemistry", Vol. 3, Marcel Dekker, New York, N.Y., 1973, p 115, and references cited therein; (g) S. Braslavsky and J. Heicklen, *Chem. Rev.*, **77**, 473 (1977).
- (6) W. J. Hehre, R. F. Stewart, and J. A. Pople, *J. Chem. Phys.*, **51**, 2657 (1969).
- (7) The CI treatment allows the mixing of 100 singly and doubly excited configurations obtained from the ground-state configuration by varying the population of the six highest occupied and the four lowest unoccupied MOs.
- (8) A. Devaquet, A. Sevin, and B. Bigot, *J. Am. Chem. Soc.*, **100**, 2009 (1978).
- (9) R. J. Cvetanovic, *Adv. Photochem.*, **1**, 134 (1963).
- (10) R. F. W. Bader, M. E. Stephens, and R. A. Gangli, *Can. J. Chem.*, **55**, 2755 (1977); O. P. Strausz, R. K. Gosavi, M. A. Robb, R. Eade, and I. G. Csizmadia, "Progress in Theoretical Organic Chemistry," Vol. 2, Elsevier, Amsterdam, 1977, p 248.
- (11) D. R. McLaughlin, C. F. Bender, and H. F. Schaffer, *Theor. Chim. Acta*, **25**, 352 (1972); J. F. Harrison, *Acc. Chem. Res.*, **7**, 378 (1974); B. O. Ross and P. M. Siegbahn, *J. Am. Chem. Soc.*, **99**, 7716 (1977); R. R. Lucchese and H. F. Schaeffer, *ibid.*, **99**, 6765 (1977).
- (12) M. A. El Sayed, *J. Chem. Phys.*, **38**, 2834 (1963); S. H. Lin, *ibid.*, **44**, 3759 (1966); T. S. Lee, *J. Am. Chem. Soc.*, **99**, 3909 (1977).
- (13) This hypothesis seems in correct agreement with the following experimental facts:^{5d} (a) there is an induction time; (b) rare gases inhibit the reaction; (c) C_2H_6 enhances the yield of acetaldehyde.
- (14) The thermodynamic values are taken from "JANAF Thermodynamical Tables," Dow Chemical Co., Midland, Mich., 1965. The heat of formation of CH_2 , from ref 5d, may be subject to caution since our final HCH angle is not the equilibrium one ($\sim 105^\circ$) for the CH_2 moiety.